Frequency Scaling of Rain Attenuation for Satellite Communication Links

Jeff D. Laster and Warren L. Stutzman, *Fellow, IEEE*

Abstract—**One year of copolarized signal data from the OLYMPUS satellite's 12, 20, and 30 GHz beacons were examined for frequency scaling of attenuation. The statistics of the ratios of attenuation in dB for the frequency pairs 30/20, 20/12, and 30/12 GHz computed at each 0.1s-sample instant were found to be nearly independent of fade depth. It was found that attenuation in dB scales with frequency to the 1.9 power. Also, attenuation ratios computed from the separate statistics of attenuation at each frequency for the same level of occurrence are very close to those found from instantaneous attenuation ratios.**

I. Introduction

RAIN attenuation is the most significant propagation mechanism for satellite communication systems operating above 10 GHz. Ku-band (14/12 GHz) is becoming heavily used, and future expansion will be toward Ka-band (30/20 GHz). Rain attenuation (in dB), however, increases approximately as the square of frequency through these bands. It is, therefore, very important to accurately predict rain attenuation for reliable incorporation into the system design process. A moderate amount of rain attenuation data are available at Ku-band, while little has been reported in Ka-band. Thus, models that permit accurate scaling of rain attenuation statistics are valuable in system design. In addition, real-time frequency scaling of attenuation can be used in adaptive fade countermeasure systems. This paper reports on measured data from an experiment at 12.5, 20, and 30 GHz. A frequency scaling model is proposed, and application to instantaneous scaling is discussed. A previous paper presented an overview of all findings [1].

Frequency scaling of attenuation is the prediction of attenuation at a desired frequency from attenuation values at another frequency. The attenuation at the base, or reference, frequency is assumed to be known from prior measurements. Many scaling models have been developed from theory, from empirical data from various propagation experiments, or from both. This paper reports on the results of an in-depth study on frequency scaling of attenuation. The investigation began with a thorough examination of one year of measured data. In addition to being useful by themselves, these results were used to evaluate the accuracy of available scaling models. Because of inadequacies in available models, new models are proposed here to more accurately reflect the measured data.

Statistical frequency scaling is the use of statistics available from prior measurements at a base frequency to predict attenuation statistics at a desired frequency. Instantaneous frequency scaling is the scaling of base frequency attenuation to predict attenuation at a desired frequency at each sample time (i.e., "instantaneously"). Virginia Tech OLYMPUS measurements demonstrate that statistical frequency scaling can be used to predict average instantaneous frequency scaling. Statistical frequency scaling facilitates the calculation of link power budgets for new systems at higher frequencies.

An alternative to the inclusion of large power margins to overcome rain fades is the use of adaptive fade countermeasures such as adaptive power control and adaptive coding (reducing data rate or adding error correction) [2]. One can increase the transmitter power as needed to compensate for fading; adjusting the earth station transmitter power is referred to as uplink power control (ULPC). Adaptive schemes allocate resources to overcome fades only as needed (i.e., as long as the fade persisted). Instantaneous frequency scaling is important in this application.

Instantaneous scaling of rain attenuation means that attenuation values measured at a base frequency in dB are scaled at each sample instant (0.1 s in the Virginia Tech experiment) for which base frequency data are available to predict attenuation values in dB at another frequency. As an example, in ULPC instantaneous scaling allows power transmitted to a satellite (i.e., on the uplink) to be varied to compensate for varying path loss where the path loss is determined by scaling from real-time attenuation data obtained at a lower frequency from the satellite to the earth (i.e., on the downlink). In addition, the move toward very small aperture antennas (VSAT) systems—having a diameter of about 1 m or less—emphasizes the need for adaptive fade countermeasures since the simplicity and small size of the VSAT's imply low system margins (e.g., margins of 3 dB are proposed). In VSAT data networks, adaptive coding is a promising technique to compensate for fading.

II. The Virginia Tech OLYMPUS Experiment

In July of 1989, the European Space Agency (ESA) launched OLYMPUS, an experimental telecommunications satellite. OLYMPUS carried four payloads to facilitate a wide range of applications which included a 12/20/30 GHz propagation payload [3]. The frequencies of the propagation

Manuscript received February 3, 1994; revised July 20, 1994.

The authors are with the Virginia Polytechnic Institute and State University, Satellite Communications Group, Bradley Department of Electrical Engineering, Blacksburg, VA 24061-0111 USA.

IEEE Log Number 9414661.

TABLE I
CHARACTERISTICS OF OLYMPUS RECEIVERS AT VIRGINIA TECH

Terminal	12	20	30
Frequency (GHz)	12.5	19.77	29.65
Polarization	Y	Switched X,Y (933 Hz)	Y
Switching loss (dB)	------	6	------
EIRP toward Blacksburg (dBW)	9.1	15.7	17.7
Antenna size (m)	4.0	1.5	1.2
Beamwidth (deg.)	0.4	0.6	0.5
C/N in 3 Hz BW (dB)	50.3	46.4	44.9

Notes:

Y = Perpendicular to equatorial plane at S/C; 51° from vertical at Blacksburg.

X = Perpendicular to Y

beacons were 12.5, 19.77, and 29.66 GHz, and are herein referred to as 12, 20, and 30 GHz.

The OLYMPUS satellite had a unique history. It left its geostationary orbit on May 29, 1991, and after seventy-six days and a trip around the world, ESA restored the spacecraft to its proper orbit and, in the middle of August 1991, turned the beacons back on. Also, in May 1992, ESA abandoned regular north–south station keeping because of low satellite fuel supply, contributing to diurnal fluctuations in satellite signal strength. OLYMPUS ceased operation in August 1993.

Under Jet Propulsion Laboratory sponsorship, the SATCOM Group of Virginia Polytechnic Institute and State University (Blacksburg, VA) constructed four earth terminals: one to receive each of the 12, 20, and 30 GHz beacon frequencies plus a second 20 GHz terminal for short baseline diversity experiments. The characteristics of the terminals are summarized in Table I. Between August 1990 and August 1992, the group made continuous measurements of the slant path attenuation on all beacon frequencies. Further details on the experiment are found in [1], [4], and [5].

The elevation angle for the Blacksburg-OLYMPUS link was 13.93 degrees. Since the lowest elevation angle in the contiguous United States for utilizing domestic geostationary satellites is about 14 degrees, these measurements represent a lower performance limit case for U.S. domestic slant path attenuation. This experiment characterizes earth–space propagation across the Ku- and Ka-frequency bands and could be the most comprehensive earth–space propagation experiment that has been performed in North America [1].

A feature of the Virginia Tech experiment which is unique in North America is the simultaneous reception of satellite signals spanning Ku-band through Ka-band from the same orbital slot. This permits direct frequency scaling. Extensive measurements have been made in the past in the Ku-band (e.g., 12 GHz), and some measurements have been taken spanning the Ka-band (e.g., 20 and 30 GHz), but very few measurements have spanned Ku- to Ka-band simultaneously (e.g., 12, 20, and 30 GHz).

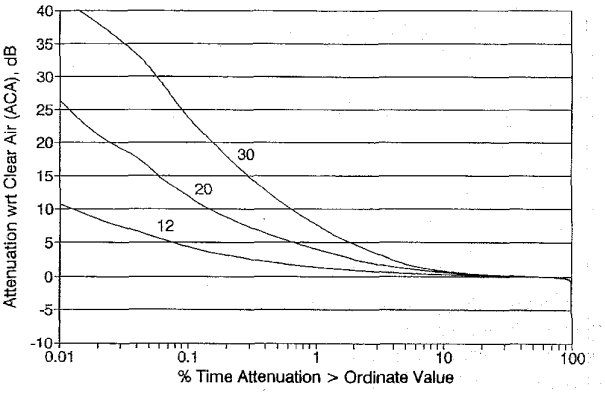

Fig. 1. Measured beacon attenuation (ACA) at 12, 20, and 30 GHz for the analysis year of January–May and September–December, 1991, and June–August, 1992. A common time base is used for all three frequencies.

Because OLYMPUS left its geostationary orbit during the summer of 1991, to obtain a full year of data for analysis purposes, June 1992 to August 1992 data are substituted for June 1991 to August 1991 in the one-year data set. Thus, the analysis year reported here consists of January–March 1991, June–August 1992, and September–December 1991.

III. STATISTICS OF ATTENUATION WITH RESPECT TO CLEAR AIR

Radiometer data were also collected at each beacon frequency along the same paths as the beacon signals. The radiometric data were used to distinguish the clear air component from the total loss, producing attenuation referenced to free space (AFS) and attenuation referenced to clear air (ACA). ACA is primarily due to rain and is, therefore, the measurement parameter used in our scaling studies. Statistical attenuation scaling is based on the statistics of ACA. The ACA statistics from the analysis year for 12, 20, and 30 GHz for their common time base (i.e., where data are present on all three frequencies simultaneously) are plotted in Fig. 1. Fig. 1 shows the percentage of time in the experiment year that ACA exceeds some specified value for the three frequencies under consideration (12/20/30). $ACAS$ used to denote the statistical ACA value exceeded for a given percentage of time. Attenuation statistics from the experiment are examined in detail in [1].

IV. INSTANTANEOUS ATTENUATION SCALING

Attenuation ratio RA is the quotient of the measured ACA value in dB at an upper frequency divided by the measured ACA value in dB at a lower frequency evaluated at each sample time t

$$RA(f_L, f_U, t) = \frac{ACA(f_U, t)}{ACA(f_L, t)}. \tag{1}$$

Each RA value is assumed to represent the entire 0.1-s sample interval. The RA values were smoothed to remove

scintillations using a 30-s moving average

$$A_{\text{ave}}(t_i) = \frac{1}{300} \sum_{j=i-150}^{i+150} A(t_j) \tag{2}$$

where t_i is the sample time. RA values were binned in increments of 0.05 for each binned 1-dB increment of the base frequency attenuation; for example, for the 30/20 GHz attenuation ratio, in a given month there might be 100 occurrences of RA values between 1.95 and 2.00 when ACA20 is between 3 and 4 dB. The statistics of RA are presented in this section.

A. RA Versus Percentage of Time Exceeded for the Analysis Year

RA occurrence times are summed and plotted cumulatively; that is, RA is plotted as a function of the percentage of time (in the month or year) that RA exceeds a specified value. Attenuation ratio RA for the analysis year for the 30/20, 20/12, and 30/12 GHz pairs are plotted in Fig. 2 for values of attenuation at the base frequency that exceed 1 dB. In this type of plot, all data are pooled regardless of base frequency attenuation level (as long as $A_{\text{ave}}(f_L) > 1$ dB).

Note that the attenuation ratio distribution in Fig. 2 is approximately constant for each of the three ratios. This is especially true for the 30/20 GHz ratio which can be approximated by a constant value of about two. This tight range of attenuation ratio values indicates potential application to adaptive control. The 50% value is the median RA value, RA_{med}, for the experiment year. RA exceeds (or is less than) RA_{med} for 50% of the time that the base attenuation exceeds 1 dB. Occurrence extremes (i.e., below about 5% and above about 95% of the time) yield relatively large and small attenuation ratios for very small amounts of time (that is, these RA values occur with low probability).

B. RA Versus Base Attenuation for the Analysis Year

All RA data are pooled regardless of attenuation level in RA exceedance plots. Binned RA values can also be plotted as a function of the base frequency attenuation for a constant percentage of time exceeded. Plotting RA as a function of base frequency attenuation reveals the dependence of RA on fade level. Yearly plots of attenuation ratios exceeding a specific value for 1, 10, 50, 90, and 99% of the time are given in Fig. 3 for the frequency ratios under consideration (30/20, 20/12, and 30/12 GHz). The percentage of time exceeded is for each 1-dB range of base frequency attenuation values (e.g., 1–2, 2–3, 3–4 dB, etc.). For example, for the 20/12 GHz pair in Fig. 3, attenuation ratio is equal to or less than 2.9 for 90% of the time that the 12 GHz attenuation is between 6 and 7 dB.

The total time base is different than that of the plots of RA versus the percentage of time exceeded. As an example, the total time base for 30/20 GHz plot of Fig. 3 is the amount of time that ACA20 exceeds 1 dB (about 1.23% of the year for this experiment) times the percentage of the year represented by 30/20 GHz common data (about 90.4% of the year), yielding a total time base of 1.11% for 30/20 GHz for the year. The 99% level of occurrence is based on this portion of the year. The 50% level of occurrence of RA, RA_{med_i}, is the median of RA for each ith 1-dB bin on the base frequency attenuation.

A linear regression was performed on the 50% level of occurrence at each 1-dB base attenuation level for $ACAS(f_U)$ versus $ACAS(f_L)$ for the experiment year. The slope of the line gives an attenuation ratio for the year averaged over the attenuation levels. This can be contrasted with Fig. 2 which pools all data without regard to attenuation level. This

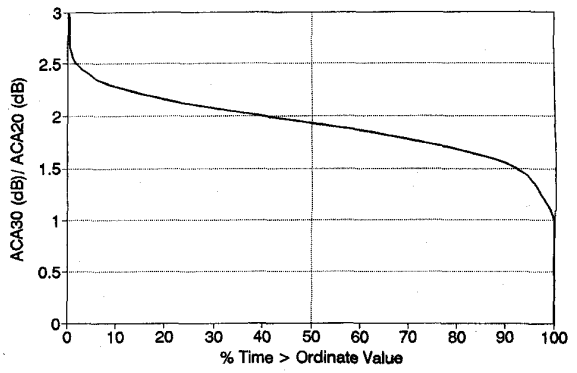

(a)

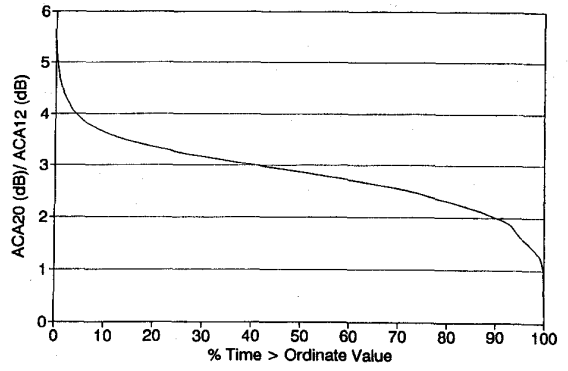

(b)

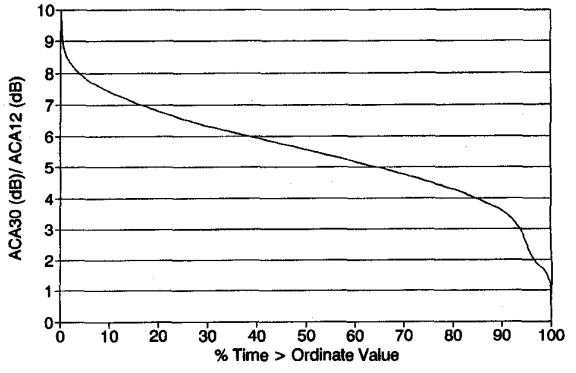

(c)

Fig. 2. RA for the analysis year as a function of the percentage of time the ordinate value is equaled or exceeded for: (a) 30/20 GHz, (b) 20/12 GHz, and (c) 30/12 GHz.

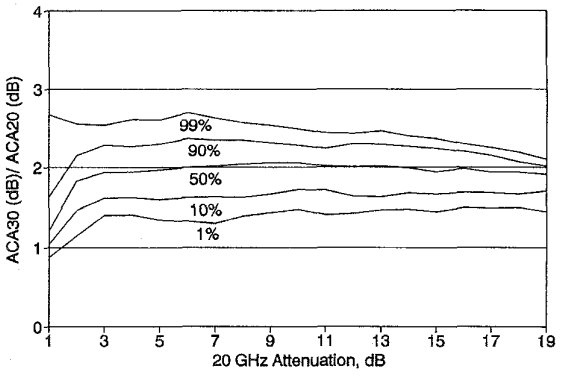

(a)

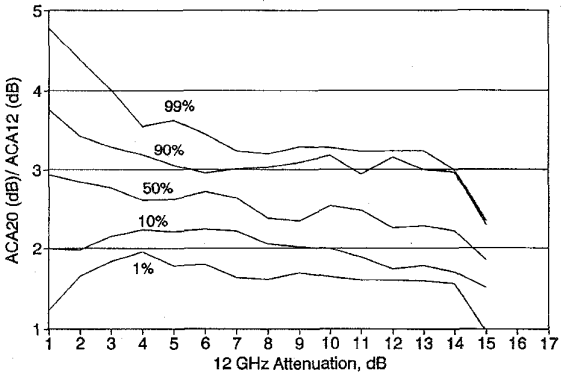

(b)

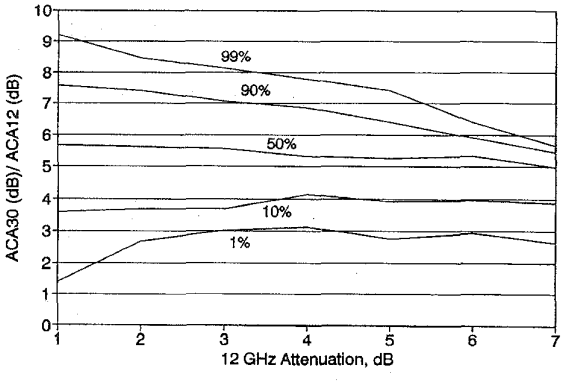

(c)

Fig. 3. RA for the analysis year as a function of the lower frequency attenuation for the frequency pairs of (a) 30/20 GHz, (b) 20/12 GHz, and (c) 30/12 GHz.

removes the heavy bias of the much more frequently occurring low attenuation levels. RA_{ave} is defined as the slope of the line obtained by linear regression. In other words, RA_{ave} is the average of the medians for 1-dB binned values of base frequency attenuation. The linear regression for the 30/20 GHz ratio has a slope of 2.01, and the standard deviation of error is 0.34 as shown in Fig. 4. Table II gives average attenuation ratio RA_{ave} from linear regressions of the 50% level for all of the frequency pairs. Table II also includes median attenuation ratio RA_{med} (from Fig. 2).

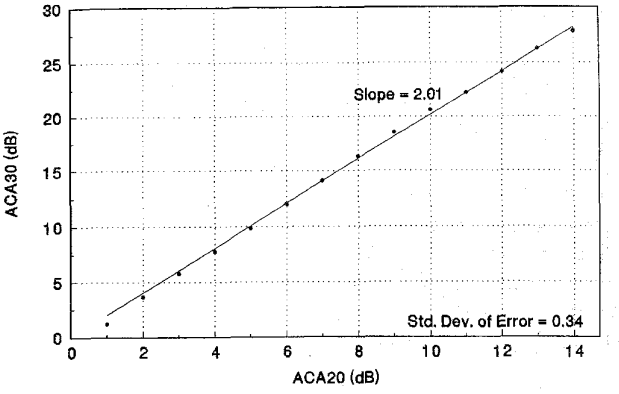

Fig. 4. Median 30-GHz attenuation for each 1-dB interval of 20-GHz attenuation using all data from the analysis year. The least mean-squared derivation straight line fit is also shown.

TABLE II
STATISTICS OF ATTENUATION RATIO FOR ONE YEAR OF OLYMPUS DATA (FOR $ACA(f_L) > 1$ dB)

Frequency Pair, f_U / f_L	30/20	20/12	30/12
Va Tech RA_{med}	1.93	2.86	5.56
Va Tech RA_{ave}	2.01	2.52	5.43
Std. Dev. of Error of RA_{ave}	0.34	0.90	0.44

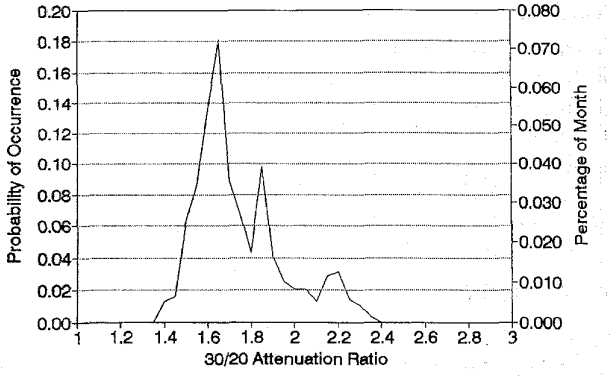

Fig. 5. Probability distribution for the occurrence of attenuation ratio at 30/20 GHz for the month of January 1991.

C. Probability of Occurrence of RA

Attenuation ratio (that is, the "instantaneous" RA value) has been observed to vary throughout a precipitation event (e.g., a hysteresis effect is documented for an individual rain event in the next section). The variation of RA with time indicates that RA is not solely a function of frequency. Some experimenters [2], [6], [7] have reported that the attenuation ratio is not constant, but few address its variability. The probability distribution function (PDF) of RA can be examined to quantify the RA variations. An example of a PDF for January 1991 is given in Fig. 5 for a base frequency attenuation greater than 1 dB for the 30/20 GHz ratio pair. In general, the PDF shows the range over which RA can vary and also shows the most probable values for RA.

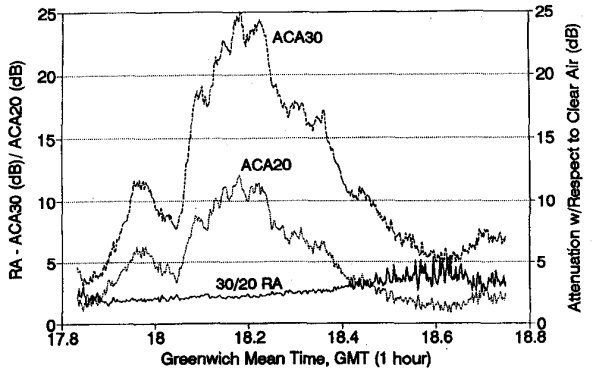

(a)

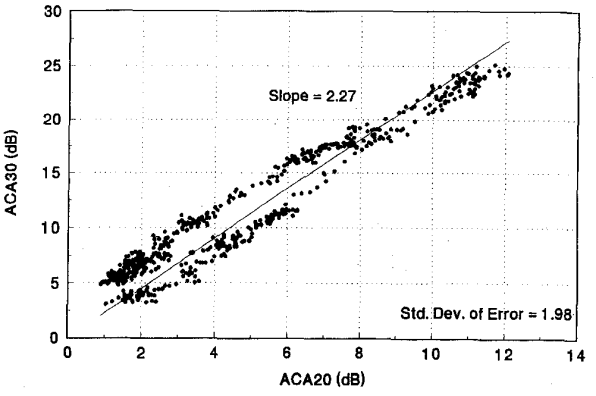

(b)

Fig. 6. Attenuation and attenuation ratio for a representative event of May 14, 1991, for the frequency pair of 30/20 GHz. (a) Attenuation and attenuation ratio as a function of time. (b) Scatter plot of attenuation at 30 GHz versus that at 20 GHz.

D. Time Variation of RA for a Representative Rain Event

Though cumulative distributions and probability distributions of RA are valuable, the time behavior of RA is often needed. A representative rain event on May 14, 1991 is shown in Fig. 6. ACA for 30 GHz and 20 GHz are plotted against each other in Fig. 6(a) (i.e., ACA30 versus ACA20, in dB). The 10-Hz sampled ACA data are averaged using the 30-s moving average of (2), and then each 50th point is plotted. A linear regression was performed to derive a "best fit" line through approximately one hour of attenuation data for the event. The slope of the line represents an average RA for the event, $RA_{\text{ave}_{\text{event}}}$, and is 2.27 for the 30/20 GHz pair.

It is interesting to examine the dynamic variations of RA during the course of the event. This type of behavior impacts directly on the utility of adaptive fade countermeasures. Attenuation ratio for 30/20 GHz for the same rain event is plotted as a function of time in Fig. 6(b) where ACA is shown for both frequencies. The data points do follow the best fit straight line, but there is an obvious spread of as much as ± 2 dB. In fact, there are two distinct clusters of points above and below the line; these clusters are associated with the late and early parts of the storm, respectively. This is known as the hysterisis effect and is due to the changing raindrop size distribution during the storm [6]. This variation in RA values is also due in part to the sensitivity of RA to small values of ACA at the base frequency.

V. Statistical Attenuation Ratio

In this section we examine statistical attenuation ratio which is defined as

$$RAS(f_L, f_U, p) = \frac{ACAS(f_U, p)}{ACAS(f_L, p)}. \tag{3}$$

RAS is the quotient of two statistical values of ACA (i.e., $ACAS$), at upper and lower frequencies, respectively, at the same percentage of time of occurrence, p. The common data base for each pair is used; that is, data are used only at instants for which attenuation pairs (A_U, A_L) are valid. RAS is a much easier quantity to obtain than RA. It is found directly from attenuation statistics in contrast to the statistics of RA which are found from instantaneous RA values for an entire period.

Plots can be generated showing the percentage of time that the statistical attenuation ratio, RAS, exceeds a specific value. RA and RAS for the year are plotted in Fig. 7 as a function of base attenuation. It should be noted that RAS values are not reliable for low base frequency attenuations $(A(f_L) < 1$ dB) because of roundoff errors (i.e., the base frequency attenuation is binned only to two decimal places in dB). To facilitate comparison, the 50% level for RA, at integer base attenuation values RA_{med_i}, are included in these plots. RAS agrees very well with the median RA for all frequency pairs, indicating attenuation statistics can be used to predict the median instantaneous ratio as a function of base frequency attenuation.

VI. Models for Frequency Scaling

A. Some Previous Models

Current models attempt to quantify the behavior of average instantaneous attenuation ratio RA_{ave} and statistical attenuation ratio RAS. Measured values of RA_{med_i} and RAS are plotted in Fig. 8 as a function of base frequency attenuation along with predictions from some of the simpler available models. This section discusses these models.

One of the most popular models is the simple power law model given by

$$RAS_n = \frac{A(f_U)}{A(f_L)} = \left(\frac{f_U}{f_L}\right)^n. \tag{4}$$

Various values of the power n have been proposed. Popular ones follow

$n = 1.8$	Dintelmann [8].
$n = 2$	Owolabi and Ajayi [9].
$n = 1.72$	Drufuca [9].

These appear as horizontal lines in Fig. 8.

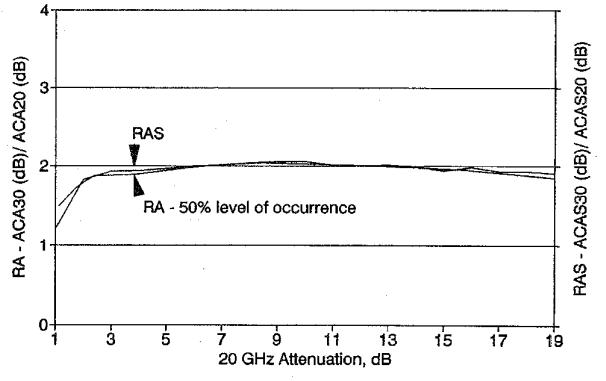

(a)

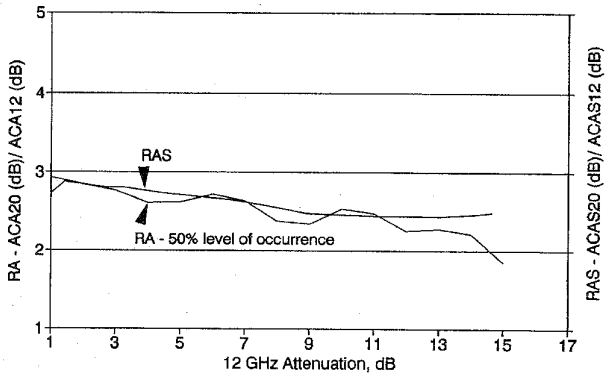

(b)

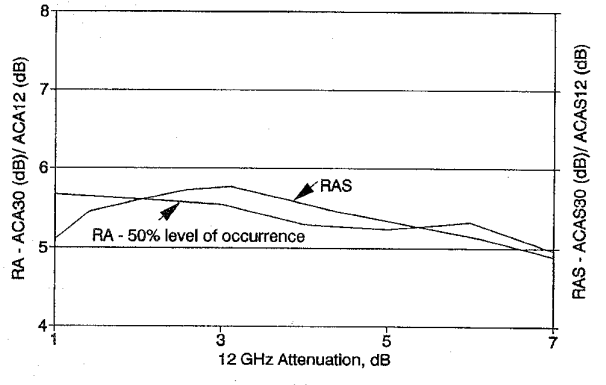

(c)

Fig. 7. Comparison of RAS to RA_{med_i} for (a) 30/20 GHz, (b) 20/12 GHz, and (c) 30/12 GHz.

There are two other models that depend only on frequency shown in Fig. 8. Battesti's model [9] is given by

$$\frac{A(f_U)}{A(f_L)} = \frac{f_U - 6}{f_L - 6} \qquad f_L, f_U \leq 20 \text{ GHz} \tag{5a}$$

$$\frac{A(f_U)}{A(f_L)} = \frac{f_U - 10}{f_L - 10} \qquad f_L, f_U \geq 20 \text{ GHz} \tag{5b}$$

$$\frac{A(f_U)}{A(f_L)} = 1.4\frac{f_U - 10}{f_L - 6} \qquad f_L < 20 \text{ GHz}, f_U > 20 \text{ GHz}. \tag{5c}$$

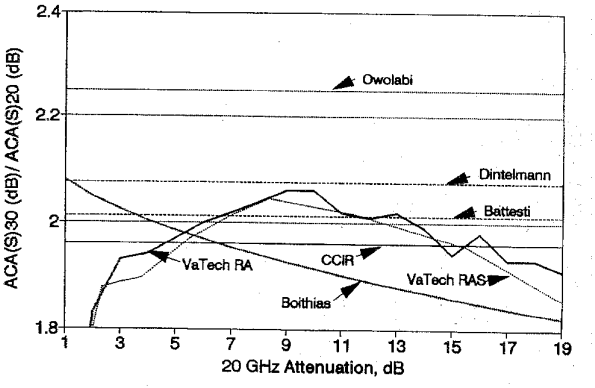

Fig. 8. Attenuation ratio for 30/20 GHz for the analysis year as a function of 20-GHz attenuation compared to several model predictions.

The International Radio Consultative Committee (CCIR) model [10] is given by

$$RAS_{\text{CCIR}} = \frac{A(f_U)}{A(f_L)} = \frac{\phi(f_U)}{\phi(f_L)}$$

where

$$\phi(f) = \frac{f^{1.72}}{1 + 3{*}10^{-7} f^{3.44}}. \tag{6}$$

A more complicated model that includes base attenuation as well as frequency is that of Boithias [11]

$$\left(\frac{A_U}{A_C}\right) = \left(\frac{\varphi_U}{\varphi_L}\right)^{1-H(\varphi_L,\varphi_U,A_L)} \tag{7a}$$

where

$$\varphi(f) = \frac{f^2}{1 + 10^{-4} f^2} \tag{7b}$$

$$H(\varphi_L, \varphi_U, A_L) = 1.12 \times 10^{-3}\left(\frac{\varphi_U}{\varphi_L}\right)(\varphi_U, A_L)^{0.55} \tag{7c}$$

and frequency f is in GHz.

Values of RA_{pred} from these models and measured data (from Table II) are compared in Table III. Missing values in the table mean that the model does not apply. Examination of Table III reveals that existing models do not satisfactorily predict either the median or average measured RA values. Some models come close for individual frequency pairs such as those of Battesti, CCIR, and Dintelmann for 30/20 GHz and Owolabi/Ajayi for 20/12 and 30/12 GHz. No models, however, are accurate across the Ku/Ka band.

B. A Proposed Law Model Based on OLYMPUS Data

The values for n computed from (4) using RA_{med} and RA_{ave} values from Table III are given in Table IV. Again, RA_{med} is the overall median RA, and RA_{ave} is the average of the medians for 1-dB binned values of base frequency attenuation. The average values of n for a power law fit over the three frequency pairs are also given in Table IV and are 1.97 and 1.90 for the median RA and average RA, respectively. The deviation from these average powers is as high as 17%. This is reasonable and leads to about a 2-dB error

TABLE III
STATISTICS OF ATTENUATION RATIO COMPARED TO MODEL PREDICTIONS FOR OLYMPUS FREQUENCIES

	Frequency pair, f_U/f_L		
Model or Data	30/20	20/12	30/12
Va Tech RA_{med} data	1.93	2.86	5.56
Va Tech RA_{ave} data	2.01	2.52	5.43
Battesti model	2.01	2.12	4.23
CCIR model	1.96	2.18	4.28
Dintelmann model	2.07	2.28	4.74
Drufuca model	---	2.20	---
Owolabi/Ajayi model	2.25	2.50	5.63

TABLE IV
POWERS, n, FOR POWER LAW FITS TO MEDIAN AND AVERAGE MEASURED ATTENUATION RATIO FOR ONE YEAR OF STATISTICS

	Powers (n) for Frequencies f_U/f_L			
Data Source	30/20	20/12	30/12	Average n
RA_{med}	1.62	2.29	1.99	1.97
RA_{ave}	1.72	2.02	1.96	1.90

out of 20 dB. Based on these results, a value of $n_{\text{ave}} = 1.90$ is recommended for 10–30 GHz frequency range

$$RA_{\text{ave}} = \left(\frac{f_U}{f_L}\right)^{1.9}. \tag{8}$$

If one is working with the frequency pairs in the OLYMPUS experiment, however, better results are obtained by using the specific power law values in Table IV.

C. Proposed Models for Attenuation Exceeded 99% of the Time

Equation (8) only predicts that average value of RA. It is important to quantify the deviation from the average behavior to assess the likelihood that an "average" model will provide accurate predictions. This can only be obtained directly from the measured data. Here we develop empirical models for 99% occurrence level of $RA, RA_{99\%_i}$, based on measured ACA values at the base frequency attenuation that exceeds 1 dB which is about 1.11% of the year for 30/20, 20/12, and 30/12 GHz. For 99% of 1.11% of the year, RA can be expected to be equal to or lower than the plotted values. This means that RA can be above what is expected for 1% of 1.11% of the year, or about 58 minutes out of a year. Furthermore, because the 99% level is for ith 1-dB bins of base frequency attenuations, the time involved is even less. For example, if the base frequency attenuation is between 9 and 10 dB on 30/20 for 60 minutes in the year (this is a high estimate), then the amount of uncertainty in RA is for only 1% of 60 minutes, or about 36 seconds in the year.

In contrast to the nearly flat 50% level plots, the 99% level plots curve downward with increasing base frequency attenuation. As long as the upper frequency attenuation is below the point where the receiver begins to saturate, this downward trend is valid. To quantify the excursions from the average behavior, second-order polynomials were fitted to $RA_{99\%_i}$ in Fig. 3. To accomplish this, $A(f_U)$ was plotted against $A(f_L)$, and the following second-order polynomial was fitted to this curve

$$A(f_U) = \alpha A(f_L) - \beta A(f_L)^2 \tag{9}$$

where $A(f_U)$ and $A(f_L)$ are attenuations at the upper and lower frequencies, and where α and β are fit coefficients. The resulting fits are

$$\text{ACA30}|99\% = 2.75 \cdot \text{ACA20} - 0.02 \cdot \text{ACA20}^2 \quad 1\text{ dB} \le \text{ACA20} \le 14\text{ dB} \tag{10a}$$

$$\text{ACA20}|99\% = 3.94 \cdot \text{ACA12} - 0.08 \cdot \text{ACA12}^2 \quad 1\text{ dB} \le \text{ACA12} \le 10\text{ dB} \tag{10b}$$

$$\text{ACA30}|99\% = 9.32 \cdot \text{ACA12} - 0.39 \cdot \text{ACA12}^2 \quad 1\text{ dB} \le \text{ACA12} \le 4\text{ dB} \tag{10c}$$

where ACA30|99%, ACA20|99%, and ACA12|99% are the 99% occurrence attenuations at 30, 20, and 12 GHz, respectively. These coefficient values are also given in Table V together with standard deviations.

TABLE V
COEFFICIENTS AND ERROR FOR MODELING 99% LEVEL RA

Ratio (Freq. Pairs)	α	β	Valid Range	Standard Dev.
30/20	2.75	0.02	1 dB ≤ ACA20 ≤ 14 dB	0.32
20/12	3.94	0.08	1 dB ≤ ACA12 ≤ 10 dB	0.93
30/12	9.32	0.39	1 dB ≤ ACA12 ≤ 4 dB	0.23

These results can be generalized to apply to any frequency pair in the Ku/Ka band range. Using the α and β values in Table V, the following general relation that approximates (10) was derived by curve-fitting through α and β and the respective values of the frequency pairs (i.e., f_U/f_L)

$$A(f_U)_{99\%} = \left(\frac{f_2}{f_1}\right)^{2.65} A(f_L) - 0.00138\left(\frac{f_2}{f_1}\right)^{6.98} A(f_L)^2. \tag{11}$$

This model yields a standard deviation of error of 0.83 dB, based on all three pairs of the Virginia Tech measured data for the experiment year. This empirical formula is very accurate for 30/12 GHz. The curve fit slightly overestimates 30/20 GHz and slightly underestimates 20/12 GHz. The deviation of these pairs is understandable considering that 20 GHz is close to a water vapor absorption band at 22.3 GHz. A higher than normal attenuation would be expected around 20 GHz which would result in (11) overestimating upper frequency attenuation for a frequency pair with the base frequency around 20 GHz. On the other hand, if the upper frequency is around 20 GHz, then (11) would underestimate the upper frequency attenuation.

As a final example, we apply the nonlinear model of (11) to the Milstar satellite frequencies of 20 and 44 GHz. A moderate

amount of attenuation data are available at 20 GHz, whereas very little are available at 44 GHz. Using these frequencies in (8) and (11) yields the following relations for the 44/20 frequency scaling ratio

$$50\%: \quad RA_{\text{ave}} = \left(\frac{44}{20}\right)^{1.9} = 4.47 \tag{12a}$$

$$99\%: \quad ACA44|99\% = 8.08 \times ACA20 - 0.34 \times ACA20^2. \tag{12b}$$

VII. Universality of Results

Since the Virginia Tech experiment is the only long-term North American measurement program to span all of the Ku/Ka-band frequencies simultaneously, it is important to speculate on its application to other situations such as different climate zones. This section addresses the application of our results to other climates and elevation angles.

Locations with a climate similar to that of Blacksburg, VA, should have similar attenuation scaling behavior. While year-to-year variation of attenuation statistics within a climate zone can be large, attenuation ratio is largely insensitive to such variations. Climate is important, however, because the variation of attenuation ratio within a rain event and rain event intensity both depend on climate. This variation seems to be due to changes in the raindrop size distribution during the rain event. For example, climate regions such as tropical areas experience more intense rainfall than is experienced in CCIR Zone K (e.g., at Virginia Tech). More intense rainfall tends to have more raindrop size distribution variation which results in attenuation ratio variations. Further research is needed in other climates to quantify RA behavior.

Attenuation statistics can be easily corrected for elevation angle change, assuming frequency is fixed. The study compared Virginia Tech's attenuation ratio statistics to that of other OLYMPUS experimenters at different elevation angles. In ratio models of attenuation scaling, there is no elevation angle dependence. Consequently, ratio models such as the power law relation of (4) are independent of elevation angle so that Virginia Tech's RA statistics can be meaningfully compared to RA statistics of other OLYMPUS experiments performed at different elevation angles.

Nonratio models, however, require elevation scaling. In contrast to ratio models, the elevation scaling factors do not cancel. This means that elevation angle scaling must be performed when applying nonratio models such as Virginia Tech's 99% models to a location with a elevation angle different from Virginia Tech's (i.e., 14 degrees).

The Virginia Tech measured data for one year and resulting proposed models were compared to those from European OLYMPUS experiments. British Telecom Labs [12] published average RA values for the OLYMPUS frequency pairs, where their average RA is slope of a best fit line through a scatter plot of $A(f_U)$ versus $A(f_L)$ for 136 rain events taken from two years of measured data. This is similar to our RA_{ave}. The results are given in Table VI. Their average RA values are less than Virginia Tech values for all frequency pairs.

TABLE VI
Comparison of Attenuation Ratio Values for Three Long Term Experiments Using OLYMPUS

	Attenuation Ratio (RA) for Frequencies f_U/f_L		
Model or Data Source	30/20	20/12	30/12
BT Labs (best fit slope of $A(f_U)$ vs. $A(f_L)$)	1.8	2.5	4.3
Dintelmann (RA computed with $n = 1.8$)	2.07	2.28	4.28
Virginia Tech Measured RA_{ave}	2.01	2.52	5.43
Power law of $n = 1.9$	2.16	2.39	5.16

Dintelmann *et al.* [8] examined one year of data from their OLYMPUS experiment in Germany and found that a power law relation with $n = 1.8$ is an adequate frequency scaling relation for the OLYMPUS frequencies. This is close to the power law relation with $n = 1.9$ derived from the Virginia Tech data. RA_{ave} scaling factors using a $n = 1.8$ power law relation are included in Table VI. Compared to Virginia Tech values, average RA values based on data from Germany ($n = 1.8$) are higher on 30/20 GHz and lower on 20/12 and 30/12 GHz.

The slight differences between European and Virginia Tech results could be due to the slight differences in climate between the localities. Attenuation ratio seems to vary with raindrop size distribution. If a location consistently experiences stratiform rain while another location experiences more thunderstorm rain, the attenuation ratio statistics are likely to differ. The statistical nature of rain events in terms of raindrop size distribution varies yearly and is difficult to quantify.

Ortgies *et al.* [13] found from the German OLYMPUS experiments that instantaneous frequency scaling of attenuation (RA) exhibits a hysteresis effect which they attribute to variations of the drop size distribution and the effective path length through rain, as well as antenna effects [14]. They maintain that the hysteresis effect begins at a much lower attenuation at 20 GHz than the 6–8 dB observed by Sweeney *et al.* [6]. The representative event of Fig. 5 displays a hysteresis effect beginning at attenuations around 1 dB.

VIII. Summary and Conclusions

This investigation explored the frequency behavior of rain attenuation over the 10–30 GHz frequency range. The study was based on measurements in Blacksburg, VA, using the 12.5, 20, and 30 GHz OLYMPUS satellite beacons. To date, and for the foreseeable future, this is the only experiment to span the entire Ku- and Ka-bands in North America. With all experiment characteristics fixed, such as elevation and azimuth angles, frequency scaling of attenuation was determined from the simultaneous beacon measurements.

Attenuation ratio is the primary quantity of interest and is the ratio of the attenuations in dB on two frequencies, upper to lower. One year of OLYMPUS data (January–May 1991, June–August 1992, September–December 1991) was examined. The study of attenuation ratio was based on the

statistics of the ratio of attenuations on two frequencies at identical instants of time.

The specific conclusions follow.

1) *The value of attenuation ratio is stable on average*: The statistics of instantaneous attenuation ratio, RA, were examined for one year. That is, the ratio of attenuations for frequency pairs 30/20, 20/12, and 30/12 were formed when valid data existed at each 0.1 Hz sample point; see (1). After smoothing using a 30s-moving average of (2) to remove scintillation effects, these data were pooled for the entire analysis year and examined for trends. The statistics were studied in two ways, by pooling all data without regard for the level of fading (see Fig. 2) and with the level of attenuation as a parameter (see Fig. 3). The median (50% occurrence level) for all data, RA_{med}, and a mean obtained by fitting a straight line at each level of attenuation, RA_{ave}, agree quite well; see Table II. This indicates the attenuation ratio on the average is stable over a year and is relatively insensitive to the depth of a rain fade. Examination of individual rain events allows more specific conclusions; see Conclusions 5) and 6) below.
2) *The nature of attenuation values from attenuation statistics at different frequencies can be used to predict the statistics of attenuation ratio*: Statistical attenuation ratio, RAS, is computed from the attenuation statistics at each frequency by taking the ratio of $A(f_U)$ and $A(f_L)$ for a common percentage of time; see (3) and Fig. 7. An important result of this experiment is that RAS tracks the 50% level of occurrence for instantaneous ratio RA, RA_{med_i}, as a function of the base frequency attenuation; that is, RAS tracks RA_{med_i}. This indicates that attenuation statistics can be used in system design to predict the median instantaneous ratio as a function of base frequency attenuation.
3) *A power law model with $n = 1.9$ fits Virginia Tech data and is proposed as a frequency scaling model*: Based on our measurements, a power law model with a power of $n = 1.9$ is recommended for scaling attenuation; see Table IV and (8). If the frequencies are close to one of the pairs in the table, that power law for that specific pair (for RA_{ave}) is more appropriate.
4) *Models for the spread of RA-measured values about the mean were developed*: Use of the constant scaling values of RA_{ave} and RA_{med} is convenient but only predicts "average" type behavior. The 99% level of occurrence of RA serves as a worst case model to quantify the deviation of RA from the average. The 99% levels of occurrence of RA for 30/20, 20/12, and 30/12 GHz depend on fade level, indicating that the relationship between the upper frequency attenuation and the lower (base) frequency attenuation cannot be well approximated by a constant attenuation ratio for these frequency pairs. Existing models are not adequate for prediction of the variation in $ACA(f_U)$ with $ACA(f_L)$. The 99% level can be approximated by a second order polynomial as given in (10) for 30/20, 20/12, and 30/12 GHz pairs.

The general model of (11) was also developed to quantify the deviation of RA for frequencies across the Ku/Ka band. This empirical formula was derived by curve fitting the empirical formula parameters from Table V (i.e., α, β, and the frequency ratio values).

5) *Attenuation ratio is relatively constant during a rain event*: The average behavior and spread about the average for one year cannot be applied to an individual rain event. At the same time, it is very important to understand the impact of rain dynamics on attenuation ratio during a rainstorm when attempting to invoke adaptive measures. This information can only be gathered through direct examination of individual events. The representative event of Fig. 6 showed that attenuation at 30 GHz versus that at 20 GHz nearly follows a straight line.
6) *Adaptive control measures can employ frequency scaling to predict attenuation*: Analysis of annual statistics as well as individual rain events indicates that an average attenuation ratio can be used to scale attenuation measured from an available beacon to another frequency where adaptive measures are to be applied [2]. The hysterisis effect, however, can lead to predictions, for example, at 30 GHz from 20 GHz that vary a few dB during a storm.
7) *Universality of results*: The largest variable in rain attenuation is that associated with the frequency of occurrence of rain. That is, different climate zones are primarily distinguished by how often it rains during a year. Attenuation ratio is insensitive to these differences, however, since it is used only when it is raining and since the character of rain tends to be somewhat universal. It is expected that good results for other climate zones and elevation angles should be obtained using the proposed power law model of $n = 1.9$. For example, the power law model with $n = 1.8$ that was found to give good results in Germany [8] would give a deviation of only 0.85 dB in the prediction of attenuation at 30 GHz (about 21 dB) from a 10 dB attenuation at 20 GHz for the $n = 1.9$ and 1.8 models.

REFERENCES

[1] W. L. Stutzman, T. Pratt, A. Safaii-Jazi, P. W. Remakius, J. Laster, B. Nelson, H. Ajaz, "Results from the Virginia Tech propagation experiment using the OLYMPUS satellite 12, 20, and 30 GHz beacons," *IEEE Trans. Antennas Propagat.*, vol. 43, no. 1, pp. 54–62, Jan. 1995.
[2] D. G. Sweeney, "Implementing adaptive power control as a 30/20 GHz fade countermeasure," in *Proc. Int. OLYMPUS Utilization Conf.*, Sevilla, Spain, Apr. 1993, pp. 623–628.
[3] B. R. Arbesser-Rastburg and G. Brussaard, "Propagation research in Europe using the OLYMPUS satellite," *IEEE Proc.*, vol. 81, pp. 865–875, June 1993.
[4] W. L. Stutzman, F. Haidara, and P. W. Remaklus, "Correction of satellite propagation data using radiometer measurements," *IEE Proc. Microwave Antennas Propagat.*, vol. 141, no. 1, pp. 62–64, Feb. 1994.
[5] R. A. Allnutt, T. Pratt, W. L. Stutzman, and J. B. Snider, "The use of radiometers in atmospheric attenuation measurements," in *IEE Proc. Microwave Antennas Propagat.*, vol. 141, no. 5, pp. 428–432, Oct. 1994.
[6] D. G. Sweeney, T. Pratt, and C. W. Bostian, "Hysteresis effects in instantaneous frequency scaling of attenuation on 20 and 30 GHz satellite links," *Electron. Lett.*, vol. 28, no. 1, Jan. 2, 1992.
[7] R. Jakoby and F. Rucker, "An overall investigation of the propagation characteristics at 12.5, 20, and 30 GHz for three specific events," in

Proc. OLYMPUS Experimenters Meeting," Darmstadt, Germany, Nov. 1993.

[8] F. Dintelmann, G. Ortgies, F. Rücker, and R. Jakoby, "Results from 12–30 GHz German propagation experiments carried out with radiometers and the OLYMPUS satellite," Research Centre, Deutsche Bundespost Telekom, Darmstadt, Germany, 1992.

[9] B. Segal, "Rain attenuation statistics for terrestrial microwave links in Canada," in "Commun. Res. Centre Rep. No. 1351-E," Ottawa, Canada, Jan. 1982, p. 14.

[10] "Attenuation by hydrometeors, in precipitation, and other atmospheric particles," in "CCIR Report 721-3, Propagation in Non-Ionized Media," vol. 5, ITU, Geneva, 1990.

[11] L. Boithias, "Similitue en frequence pour l'affaiblissement par la pluie," *Ann. Telecommun.*, vol. 44, no. 3–4, pp. 186–191, 1986.

[12] R. G. Howell, R. L. Stucky, and J. W. Harris, "The BT Laboratories slant-path measurement complex," *BT Technol. J.*, vol. 10, no. 4, Oct. 1992.

[13] G. Ortgies, F. Rücker, and F. Dintelmann, "Some aspects of attenuation frequency scaling," in *Proc. North American Radio Sci. Meeting Int. IEEE/AP-S Symp.*, London, Canada, 1991.

[14] G. Ortgies, F. Rücker, F. Dintelmann, and R. Jakoby, "Effect-specific analysis of propagation parameters," in *Proc. 16th NASA Propagat. Experimenters Meeting (NAPEX XVI) ACTS Propagat Studies Miniworkshop,* Houston, 1992, pp. 143–154.

Jeff D. Laster received the B.S. and M.S. degrees in electrical engineering from Virginia Tech in 1991 and 1993, respectively. He also received the B.A. degree in humanities in 1985. He is currently pursuing his Ph.D. in electrical engineering at the Virginia Polytechnic Institute, Blacksburg, VA, as a recipient of a Bradley Fellowship and a DuPont Fellowship.

His current research interests include single-channel interference rejection techniques in wireless digital communications systems and also demodulation techniques.

Warren L. Stutzman (S'63–M'69–SM'77–F'89) received the B.S. degree in electrical engineering and A.B. degree in mathematics degrees from the University of Illinois, Urbana-Champaign, in 1964 and the M.S. and Ph.D. degrees in electrical engineering from Ohio State University, Columbus, OH, in 1965 and 1969, respectively.

In 1969 he joined the electrical engineering faculty of Virginia Polytechnic Institute and State University where he is currently the Thomas Phillips Professor of Engineering. He is Director of the Satellite Communications Group and the Antenna Laboratory at Virginia Tech which are part of the Center for Wireless Telecommunications. In 1983 he was a Visiting Professor at the Physical Science Laboratory of New Mexico State University. His research interests include antenna design, reflector antennas, phased array antennas, personal communication systems, atmospheric effects on earth-space communication links, and microwave measurements of vegetation. He is coauthor with Gary A. Thiele of the textbook *Antenna Theory and Design,* (John Wiley, 1981) and is author of the book *Polarization in Electromagnetic Systems,* (Artech House, 1993).

Dr. Stutzman has held the following offices in the Antennas and Propagation Society: Administrative Committee from 1984–1986, Chairman of the AP-S Meetings Committee from 1988–1991, Vice President for 1991, and President for 1992.